

## PREDICTION OF THERMAL PERFORMANCE OF DESIGNED DIFFERENT OBSTACLES ON ABSORBER PLATES IN SOLAR AIR COLLECTORS BY SUPPORT VECTOR MACHINE

*Fatih KOÇYİĞİT<sup>1</sup>, Vedat Veli ÇAY\*<sup>1</sup>, Ömer Osman DURSUN<sup>1</sup>, Ebru Kavak AKPINAR<sup>2</sup>*

<sup>1</sup>Civil Aviation School, Dicle University, 21280, Diyarbakır, Turkey

<sup>2</sup>Mechanical Engineering Department, Fırat University, 23279, Elazığ, Turkey

\* Corresponding author; vedatcay@yahoo.com

*In this study, energy performance of a new flat plate solar air collector (SAHs) with different obstacles at fin shape and rectangle Type I and Type II was investigated. The measured parameters were the inlet and outlet temperatures, the absorbing plate temperatures, the ambient temperature, and the solar radiation. Further, the measurements were performed at different values of mass flow rate of air (0.0074, 0.0052, 0.0016 kg/s). The thermal efficiency was calculated based on the measurements. The results obtained were trained and tested with the support vector machine (SVM) which is one of the regression analysis methods. 10-fold cross-validation method was used to evaluate the regression performance. The best regression analysis result was obtained using cubic SVM method in which  $R^2$  was 0.88 in the Type II air collector. Comparison between predicted and experimental results indicates that the proposed SVM model can be used for estimating the efficiency of SAHs with reasonable accuracy.*

Keywords: Solar Air Collector, Thermal Efficiency, SVM

### 1. Introduction

The energy transferred to the Earth in a year from the Sun, which is accepted as an endless source of energy for the world, is more than 150 times the energy of the coal reserves available in the World [1]. In recent years, the idea of benefiting from this clean and everlasting source of energy as much as possible has attracted the attention all over the world, especially in the countries that are located between 45° north and south latitudes and called as the Sunbelt in which our country is also included. Although our country is located in a region that is rich in solar energy and called as the sunbelt, solar energy cannot be benefited sufficiently. It has been determined that the average annual total sunshine duration of our country is 2640 hours (a total of 7.2 hours per day) and the average total radiation intensity is 1311 kWh/m<sup>2</sup>-year (a total of 3.6 kWh/m<sup>2</sup> per day) [2].

The use of air-heating method, which is another form of benefiting from solar energy, has also begun to gain importance. The SACs are generally used for space heating and the drying of agricultural products. Nowadays, intensive studies are carried out to make many changes and improvements on traditional systems with the aim of increasing the low efficiency of plane collectors that are commonly used in air heating, which is the major disadvantage of them in air heating. The use of selective surface

is one of them. An attempt to increase the amount of absorbed solar radiation is made with the use of selective surfaces having high absorption coefficient and low emissivity coefficient [3-5]. Another method applied to increase the efficiency of air heaters is to increase the number of passages of air through the absorber plate. Thus, the duration of the air in the collector is increased, so more heat absorption is ensured [6,7]. Another improvement applied to increase the efficiency is to increase the surface on which the solar radiation is absorbed by giving a rough appearance to the absorber plate and to ensure the further contact of the air that passes through with this surface [8,9]. The placement of the fin on the absorber surface to increase the heat transfer is another improvement method that is attempted to increase the collector's efficiency. It has been ensured that the total heat transferred and thus the efficiency have been increased by increasing the heat transfer area of the air with these fins that are frequently placed in the flow channel [10].

In the literature, many arrangements have been proposed to improve the heat convection coefficient between the absorber plate and the air. The replacement of the absorber plate form is also one of the performance improvement methods. Aldabbah et al. used the wire mesh structure as the fluidized bed in single and double pass solar air collectors and experimentally tested its performance. They observed that the thermal efficiency was significantly increased with the wire mesh structure compared to the flat absorber plate solar collectors with conventional structure [11]. Yeh et al. carried out a study on the collector efficiency of air heaters on and under the absorber layer during air flow [12]. Karim and Hawlader experimentally and theoretically investigated flat-layer, finned and v-curved air heaters to improve the performance of conventional air heaters to improve the performance of conventional air heaters [13]. Hachemi experimentally examined the thermal performance by placing offset fins on the absorber plate [14]. Esen performed the energy and exergy analysis by placing the barriers in different shapes on both sides of the absorber plate in the solar air collector. In his study, he stated that the thermal performance according to the shape of the barriers was improved compared to the flat absorber plate condition [15]. Esen et al. experimentally examined the thermal efficiency of a solar-powered air collector and created the support vector machine model of the system [16].

Superior generalization performance is obtained from SVM regression and more importantly, the performance does not depend on the dimensionality of the input data. The SVM is derived from the statistical learning theory [17], and is a two-layer network with the inputs transformed by the kernels corresponding to a subset of the input data. The output of the SVM is a linear function of the weights and the kernels. The weights and the structure of the SVM are obtained simultaneously by constrained minimization for a given precision level of the modelling error. In the constrained minimization, kernels corresponding to data points that are within the error bounds are removed. The support vector regression (SVR) is formed by the retained kernels [18], and the data points associated with the retained kernels are referred to as the support vectors (SVs). Since the kernels of the SVR are similar to the basis functions of the radial basis function (RBF) network with scatter partitioning, it is shown here that the SVR can be reformulated as a RBF network with basis functions normalized such that they form a partition of unity [19].

In this study, a new absorber plate to ensure increase in thermal efficiency was designed. The thermal efficiency of the designed collector was found and compared both experimentally and with the SVM model.

## 2. Material and Method

In this study in which the energy analysis of a newly developed planar type air solar collector was performed, the upper part of the absorber plate containing fin arranged at 2 different types, positions and angles and barriers in the form of a rectangular block was painted black and covered with copper sheet (Figure 1). A constant-speed fan ( $0.0833 \text{ m}^3\text{s}^{-1}$ , 0.25 kW, 220 V, 50 Hz,  $1380 \text{ min}^{-1}$ ) was used to blow the air used in the system. The airflow of the fan can be adjusted by means of the valve in the fan inlet. The experiments were performed in Elaziğ province in July and August of 2007 (the period between July 05, 2016 - August 10, 2007).

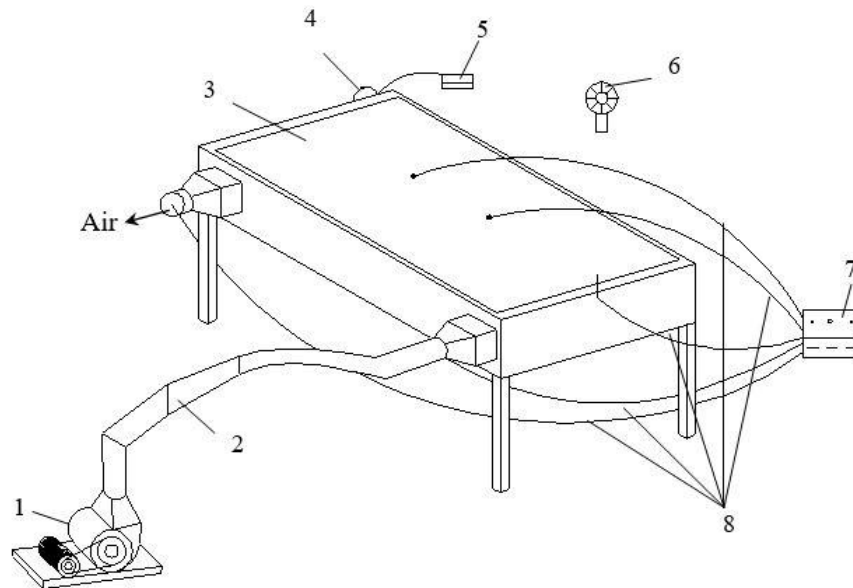


**Figure 1.** Schematic representation of the experimental set [1]

- 1) Radial Fan, 2) Connecting pipe, 3) Planar type air solar collector, 4) Pyranometer, 5) Solar integrator, 6) Anemometer, 7) Digital thermometer and channel selector, 8) Thermocouples



**Figure 2.** Side view of the experimental set [1]

As it is seen in Figure 2, air collectors are 120x70x12 cm in size, and 16x5x7 cm channels that provide the inlet and outlet of the air to the solar collector were longitudinally opened on both sides (12cm section). The absorber surface that absorbs the solar radiation, which is the most important element of the collector, was made of blacked galvanized steel. The fins in different geometric shapes and arrangement and the barriers in the form of a rectangular block were placed to ensure the circulation of air on the absorber surface for a long time and thus to increase the heat transfer surface. These barriers were used to increase the heat transfer surface and path, as it is also seen in the following figures. In this study, the absorber surface on which there were barriers in the form of a rectangular fin was defined as the Type 1, and the absorber surface on which there were barriers in the form of leaf fin was defined as the Type 2. In addition to the fin-shaped barriers on Type 1 and Type 2 absorber surfaces, 10 cm high, 50 cm long and 2 cm thick barriers in the form of a rectangular block were also placed for the air circulating inside to follow a wave motion path and therefore to remain in the collector for longer. The photograph of the absorber surfaces defined as Type 1 and Type 2 is presented in Figure 3 (a, b).

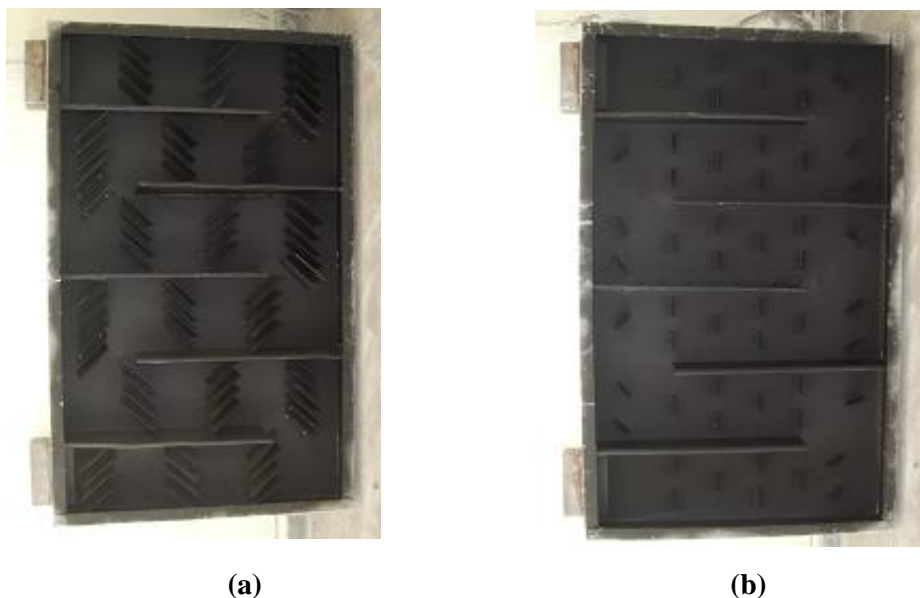


**Figure 3.** Photographs of the absorber plate surfaces **a)** Rectangular fin-type absorber (Type 1) **b)** Leaf-fin type absorber (Type 2)

The experiments were performed between the period of July 05, 2016 - August 10, 2016. The experiments were started at 9:00 a.m and ended at 17:00 p.m. In the experiments, the flow rate was adjusted by the valve at the outlet of the fan so that the mass flow of the air would be 0.0074 kg/s, 0.0052 kg/s and 0.0016 kg/s. During the experiments, the inlet temperature of the air to the collector, its outlet temperature from the collector, the temperature of the absorber surface, outside ambient air temperature, the wind speed and the solar radiation values were measured at 10 minute intervals.

### 2.1. Thermal Efficiency Analysis

Thermal efficiencies of solar power planar collectors are dependent on the optical and thermal efficiencies of the absorber surface and external climate characteristics (temperature and wind speed), the angle of incidence of solar radiation, the solar radiation to the collector plane, the inclination of the collector and the mass flow of the working fluid.

The instantaneous thermal efficiency of solar powered planar collectors is defined as the ratio of useful radiation from the working fluid to the solar energy coming to the collector surface.

$$\eta = \frac{\dot{Q}_c}{A.I} \quad (1)$$

Here;  $\eta$ : thermal efficiency,  $\dot{Q}_c$ : useful heat, A: collector area ( $m^2$ ) and I: total solar radiation intensity coming to the unit area of the collector plane ( $W/m^2$ ). The useful heat ( $\dot{Q}_c$ ) is expressed by the following equation.

$$\dot{Q}_c = \dot{m}C_p(T_{\zeta} - T_g) \quad (2)$$

Here;  $\dot{m}$ : mass flow of the working fluid (kg/s),  $C_p$ : specific heat of the working fluid ( $J/kg^{\circ}C$ ),  $T_{\zeta}$  and  $T_g$ : are the outlet temperature of the working fluid from the collector and the inlet temperature to the collector, respectively ( $^{\circ}C$ ). The incoming solar energy, the useful heat, and the heat losses to the environment are determined using the measurement values taken for the thermal efficiency experiments of the planar solar collector. The thermal efficiency of a planar collector operating in steady-state conditions is defined in average fluid temperature as the following;

$$\eta = F_m(\tau\alpha) - F_m U(T_f - T_e)/I \quad (3)$$

Here;  $F_m$ : is defined as the ratio of the useful heat that is actually obtained from the collector to the useful heat that can be obtained if the entire collector surface is at the fluid average temperature and is called as the collector thermal efficiency factor, U: total heat loss coefficient ( $W/m^2^{\circ}C$ ),  $T_e$ : ambient temperature ( $^{\circ}C$ ),  $\tau$ : glass cover permeability coefficient and  $\alpha$ : absorption coefficient of the absorber surface.

The average temperature of the working fluid ( $T_f$ ) is taken as the average of the fluid inlet and outlet temperatures.

$$T_f = (T_{\zeta} + T_g)/2 \quad (4)$$

It is assumed that the total heat loss coefficient is constant in the formation of collector thermal efficiency curves by using a linear approach. However, the total heat loss coefficient in the thermal efficiency equations described above is not constant, and the absorber surface, the temperatures of the environment and sky, wind speed and the inclination of the collector are dependent on the properties of the absorber surface. The effect of these variables on the collector heat loss coefficient and therefore on the collector thermal efficiency has not been examined in detail. In the relevant standards that are currently in force in Turkey, there is not any efficiency evaluation experiment except for the limit values such as the fact that the wind speed is below 5.5 m/s and the ambient temperature is between 5-32 $^{\circ}C$ . The collector thermal efficiency equation is given by the second-degree equation based on the average fluid temperature (4) equation by taking into account the change of the total heat loss coefficient in the new Turkish standards in Turkey prepared in compliance with the European standards.

$$\eta = F_m(\tau\alpha) - \alpha_1(T_f - T_e)I - \alpha_2 I[(T_f - T_e)I]^2 \quad (5)$$

Here;  $\alpha_1$ : the first-degree heat loss coefficient,  $\alpha_2$ : the second-degree heat loss coefficient. The  $\alpha_2$  value should not be negative to be able to express the thermal efficiency with the second degree equation. In addition, the radiation value should be 800  $W/m^2$ . If the new approach and the currently used evaluation

method are compared, there may be differences according to the results to be obtained from the linearized thermal efficiency curve of the equilibrium temperature and optical efficiency values [20].

## 2.2. Support Vector Machine (SVM)

SVM is one of the machine learning algorithm methods used to separate one or more classes from each other [21]. The purpose in SVM is to find the hyperplane that will most appropriately separate the classes in the data from each other. Let the plane to separate the data in the training set is  $w \cdot x + b$ . Here, the normal of the hyperplane is  $w$  and  $b$  is the bias, in other words, the constant value.

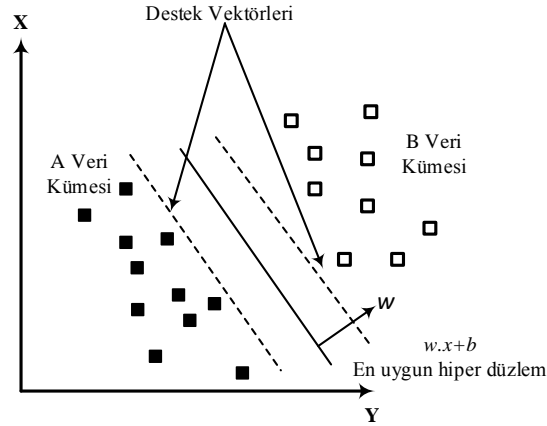


**Figure 4.** The best hyperplane that is capable of separating the data

As it is seen in Figure 1, many different planes can be used to separate the classes in the data set. It is the purpose of the SVM to be able to separate the classes from among these planes and to find the planes that make the distance between them greatest. For this, all the data in the dataset should ensure the following equation.

$$y_j(w^T x_j + b) \geq 1 \quad \forall x_i \quad (6)$$

For the specified hyperplane to be maximum

the expression  $\frac{1}{2} \|w\|^2$  should be the smallest [21,22]. Lagrange multipliers are used to solve this quadratic problem.

$$L = \frac{\|w\|^2}{2} - \sum_{j=1}^m \alpha_j [y_j(w^T \cdot x_j + b) - 1] \quad (7)$$

As a result, the decision function that will be used to separate the two classes

$$f(x) = \text{sign} \left( \sum_{j=1}^m y_j \alpha_j (x \cdot x_j) + b \right) \quad (8)$$



The SVM uses various kernel functions (linear, rbf (radial basis function), polynomial) to linearly separate the data set. These kernel functions are shown below [21-24].

$$\text{Linear: } K(x, y) = (x \cdot y) \quad (9)$$

$$\text{RBF: } K(x, y) = \exp\left(-\frac{\|x - y\|^2}{2\sigma^2}\right) \quad (10)$$

$$\text{Polynomial: } K(x, y) = (x \cdot y + 1)^d \quad (11)$$

Here,  $\sigma$ ,  $d$  are the parameters belonging to kernel functions.

In the regression analysis, the Root Mean Square Error (RMSE) is calculated. The fact that this value is as small as possible indicates that the regression analysis has given a good result. One of the important statistical values in regression analysis is the R2 value. The R2 value takes values between 0 and 1. The fact that the R2 value is found to be 0 or close to 0 shows that the prediction result obtained in the regression analysis is bad, and the fact that it is found to be 1 or close to 1 shows that the regression analysis has given a good result. The mathematical expression of RMSE and R2 is seen in equations 7 and 8 [25-27].

$$RMSE = \sqrt{\frac{1}{n} \sum_{i=1}^n (y_i - y'_i)^2} \quad (12)$$

$$R^2 = 1 - \frac{\sum_{i=1}^n (y_i - y'_i)^2}{\sum_{i=1}^n y_i^2} \quad (13)$$

$n$ : is expressed as the number of samples in the independent variable dataset

$y_i$ :  $i$ . is expressed as the measured output value of the data

$y'_i$ :  $i$ . is expressed as the estimated output value of the data [25-27].

### 2.3. Cross Validation

Cross validation is one of the statistical methods that evaluate the data set in two parts, the training and the test set. One of the cross validation methods is the  $k$ -part cross validation method. In this method, the data set is divided into  $k$  pieces. While the  $k-1$  piece is used as the training data, the other piece is used as the test data. The same operation is applied for all pieces. Thus, the whole data set is used for both training and testing. The average of the accuracy rates of the obtained test data is taken [28-30].

### 3. Results and Conclusions

The data obtained from the Type I air collector were evaluated with SVM, which is one of the regression learning methods. As it is seen in Figure 5.a, it was observed that the Linear SVM, in which

the samples of the Type I air collector were distributed close to the linear line that is considered to be the best estimate, gave a good result. The Good Gaussian and Intensive Gaussian SVM, in which the samples seen in Figure 5.d and Figure 5.f were distributed distantly to the linear line, gave a bad result. In the evaluation of the regression analysis, the situation where the Root Mean Square Error (RMSE) value is closest to zero and the statistical value  $R^2$  is closest to 1 is the situation where the best estimation is performed. When the data of the Type I collector in Table 1 were examined, it was seen that the Linear SVM, in which the  $RMSE$  value was closest to zero by 0.04 and the  $R^2$  value was closest to 1 by 0.74, gave a good result. In addition to this, the Good Gaussian and Intensive Gaussian SVM, in which the  $RMSE$  was found to be 0.06 and the  $R^2$  value was found to be 0.37, gave the worst result for Type I collector. When Figure 6.c including the samples of the Type II air collector was examined, the Cubic SVM, in which the samples were distributed close to the linear line, gave a good result. When the samples in Figure 6.d were examined, it was seen that the Good Gaussian SVM, in which the samples were distributed distantly to the linear line, gave a bad regression result. When the  $RMSE$  and  $R^2$  values of the Type II collector in Table 2 were considered, the Cubic SVM, in which the  $RMSE$  was found to be 0.03 and the  $R^2$  value was found to be 0.88, gave a good result. The Good Gaussian SVM, in which the  $RMSE$  and the  $R^2$  value of the Type II collector in Table 1 were found to be 0.07 and 0.48 respectively, gave a bad result. When the data of both types of collectors in Table 1 were evaluated, the Cubic SVM method, in which it was attempted to estimate the collector type using the data of the Type II collector type, gave the best regression analysis result.

## References

- [1] Koçyiğit H., Yutucu plaka üzerine farklı türde kanatçıkların yerleştirildiği bir havalı kollektörün enerji ve ekserji analizi, Yüksek Lisans, Fırat Üniversitesi, 2008.
- [2] Güneş Enerjisi Potansiyel Atlası, (2007). [www.eiei.gov.tr](http://www.eiei.gov.tr)
- [3] Karsli, S., Performance analysis of new-design solar air collectors for drying applications, *Renewable Energy*, 32, (2007), pp.1645-1660.
- [4] Ucar, A., Inallı, M., Thermal and exergy analysis of solar air collectors with passive augmentation techniques, *International Communications in Heat and Mass Transfer*, 33 (2006), pp. 1281–1290.
- [5] Moummi, N., Youcef-Ali, S., Moummi, A., Desmons, J.Y., Energy analysis of a solar air collector with rows of fins, *Renewable Energy*, 29, (2004), 13, pp. 2053-2064.
- [6] Hegazy Adel, A., Optimization of flow-channel depth for conventional flat-plate solar air heaters, *Renewable Energy*, 7, (1996) 1, pp.15-21.
- [7] Dincer, I., On energetic, exergetic and environmental aspects of drying systems, *International Journal of Energy Research*, 26 (2002), 8, pp.717-727.
- [8] Dincer, I. and Sahin, A.Z., A new model for thermodynamic analysis of a drying process, *International Journal of Heat and Mass Transfer*, 47 (2004), 4, pp.645-652.
- [9] Midilli, A., Kucuk, H., Energy and exergy analysis of solar drying process of Pistachio, *Energy*, 28, (2003) pp. 539-556.
- [10] Kurtbas, İ., Durmuş, A., Efficiency and exergy analysis of a new solar air heater, *Renewable Energy*, 29, (2004), pp. 1489-1501.
- [11] Aldabbagh L.B.Y., Egelioglu, F., Ikan M., Single and double pass solar air heaters with wire mesh as packing bed, *Energy*, 35, (2010) pp. 3783–3787.
- [12] Yeh, H., Ho, C., Hou, J., The improvement of collector efficiency in solar air heaters by simultaneously air flow over and under the absorbing plate, *Energy*, 24, (1999), 857-871.



- [13] Karim, Md. A., Hawlader, M.N.A., Performance investigation of flat plate, v-corrugated and finned air collectors, *Energy*, 31, (2006), pp. 452-470.
- [14] Hachemi A., Experimental study of thermal performance of offset rectangular plate fin absorber-plates, *Renewable Energy*, 17 (1999) 3 pp. 371–84.
- [15] Benli, H., Determination of thermal performance calculation of two different types solar air collectors with the use of ANN, *Int. Jo. of Heat and Mass Transfer*, 60, (2013) pp. 1-7.
- [16] Esen H., Özgen F., Esen M., Sengür A., Artificial neural network and wavelet neural network approaches for modelling of a solar air heater, *Expert System with Applications*, 36, (2009), pp. 11240-11248.
- [17] Zhong, Z. D., Zhu, X. J., and Cao, G. Y., Modeling a PEMFC by a support vector machine. *Journal of Power Sources* 160 (2006) 1, pp. 293–298.
- [18] Drezet, P. M. L., and Harrison, R. F., Support vector machines for system identification, *UKACC International Conference on CONTROL '98, 1–4 September (1998)*, pp. 688–692.
- [19] Schölkopf, B., Sung, K., Burges, C. J. C., Girosi, F., Niyogi, P., Poggio, T., and Vapnik, V.N. Comparing support vector machines with gaussian kernels to radial basis function classifiers. *IEEE Transactions on Signal Processing* 45, (1997) pp. 2758–2765.
- [20] Yıldız , A., Gürlek, G., Güngör, A., ve Özbalta, N., Alüminyum ve Bakır borulu Güneş Kolektörlerinin Enerji ve Ekserji Verimlerinin Deneysel Karşılaştırılması, *Mühendis ve Makine* Cilt: 48,(2002) Sayı: 569
- [21] Khazae, A., Ebrahimzadeh, A., Classification of electrocardiogram signals with support vector machines and genetic algorithms using power spectral features, *Biomedical Signal Processing and Control*, 5, (2010) 4, pp. 252–263.
- [22] Ayhan, S., Erdoğan, Ş., Destek Vektör Makineleriyle Sınıflandırma Problemlerinin Çözümü İçin Çekirdek Fonksiyonu Seçimi, *Eskişehir Osmangazi Üniversitesi İİBF Dergisi*, 9, (2014) 1, pp. 175–198,
- [23] Osuna, E., Freund, R., Girosi, F., Support Vector Machines: Training and Applications, *Massachusetts Institute of Technology*, 9217041 (1997), no. 1602.
- [24] Mehta, S.S., Lingayat, N.S., Development of SVM based classification techniques for the delineation of wave components in 12-lead electrocardiogram, *Biomedical Signal Processing and Control*, 3, (2008) 4, pp. 341–349.
- [25] Chatterjee, S., A. S., Hadi, Regression Analysis by Example, 5th ed. Hoboken: John Wiley & Sons, 2012.
- [26] Diez, D.M., Barr, C.D., Çetinkaya-Rundel, M., OpenIntro Statistics Third Edition, 2nd ed. OpenIntro, 2012.
- [27] Esen, H., Ozgen, F., Esen, M., Sengur, A., Modelling of a new solar air heater through least-squares support vector machines, *Expert Systems with Applications*, 36, (2009) 7, pp. 10673–10682.
- [28] Akbari, A., Arjmandi, M. K., An efficient voice pathology classification scheme based on applying multi-layer linear discriminant analysis to wavelet packet-based features, *Biomedical Signal Processing and Control*, 10, (2014) 1, pp. 209–223.
- [29] Wong, T.T., Performance evaluation of classification algorithms by k-fold and leave-one-out cross validation, *Pattern Recognition*, 48, (2015) 9, pp. 2839–2846
- [30] Jiang, G., Wang, W., Error estimation based on variance analysis of k-fold cross-validation, *Pattern Recognition*, 69, (2017), pp. 94–106.